Defect Production and Annealing in Ion-Implanted Amorphous Silicon

S. Coffa, F. Priolo, and A. Battaglia
Dipartimento di Fisica, Università di Catania, Corso Italia 57, 195129, Catania, Italy
(Received 23 December 1992)

We have elucidated the mechanisms of defect production and annealing in ion-implanted amorphous silicon using *in situ* conductivity measurements as a probe of the defect structure. The defect evolution is shown to depend strongly on the substrate temperature and slightly on the irradiating ion and dose rate. It is demonstrated that two different defect structures exist, one of which, never observed before, is stable at 77 K and anneals out upon heating to 300 K. These results are explained on the basis of a new model of defect evolution in amorphous silicon.

PACS numbers: 61.80.Jh, 68.60.Dv, 72.80.Ng

Thermal annealing of ion-implanted amorphous silicon (*a*-Si) produces modifications of the vibrational [1,2], optical [3], and electrical [4,5] properties of the material. These modifications are usually referred to as structural relaxation. Recent investigations using calorimetry [2,6, 7] and metal diffusion [8] have shown that structural relaxation can be interpreted in terms of defect annihilation and concomitant bond rearrangement. The concentration of these defects can be reduced by a factor of ~ 5 upon annealing at ~ 800 K [2,8] of the as-implanted material. Moreover the process can be reversed by reimplanting a previously annealed material [5,9]. The annealing kinetics of these defects demonstrates [2] that different defect structures are present in *a*-Si. Dangling bonds [10], floating bonds [11], strained Si-Si bonds [12], and vacancy-like defects [13] have been so far suggested.

In spite of this huge number of experimental investigations several points are still unclear. In particular, the mechanisms of defect production and dynamic annealing during ion bombardment are not understood. These represent crucial information for the description of a variety of nonequilibrium phenomena occurring under ion irradiation, such as ion-induced epitaxial crystallization [14], ion-assisted nucleation [15,16], and radiation-enhanced diffusion [17]. Moreover the defect annihilation kinetics below room temperature is unknown, making it impossible to provide a complete description of the defect structure of *a*-Si. These limitations are mainly due to the lack of direct experimental evidences as most of the analyses have been performed *ex situ*, after irradiation and heating of the sample to room temperature (RT).

Recently, *in situ* techniques have been shown to represent a powerful tool for the investigation of the *a*-Si structure and evidenced the existence of structural relaxation phenomena below room temperature [4,5,18,19]. In this Letter we make use of *in situ* conductivity measurements to explore dynamic defect accumulation during ion bombardment and the early stages of structural relaxation following irradiation. Moreover, evidence for dramatic defect annihilation upon heating from 77 K to RT is provided. These experimental data allow us to embody in a new comprehensive model the effect of ion beam irradiation in *a*-Si.

Amorphous Si layers, 0.33 μm thick, were deposited by low pressure chemical vapor deposition at 813 K on 1.3 μm thick oxide layers thermally grown onto Si substrates. Following deposition the material was implanted with Si at an energy of 300 keV to a fluence of 5×10^{15} ions/cm^2 to destroy any eventually preexisting crystalline nucleus. The samples were then fully relaxed by annealing at 813 K for 1 h. Aluminum patterns, 1 μm thick, were photolithographically defined on the samples. These patterns consist of two Al stripes 80 μm apart, having a total perimeter of 7.8 cm. A two-point probe configuration was used for the measurements. *In situ* conductivity measurements were performed during irradiation with 2.0 MeV Si ions and 7.0 MeV Au ions at 77 or at 300 K.

Electronic transport in *a*-Si in the temperature range between 300 and 77 K occurs by the hopping mechanism [4,20,21]. Conductivity measurements in *a*-Si are then particularly sensitive to those defects introducing deep-lying states in the band gap. The conductivity is given by [20]

$$\sigma=\sigma_0\exp[-(T_0/T)^{1/4}], \quad (1)$$

where

$$T_0=\frac{16\alpha^3}{k_B g(E_F)}, \quad (2)$$

α^{-1} being the localization of the electron wave function, k_B the Boltzmann constant, and $g(E_F)$ the density of states (DOS) at the Fermi level, which is proportional to the density of defects. Assuming a typical value of 3 Å for α^{-1} [20] and using the measured value of 8.4×10^5 Ω^{-1}cm^{-1} for σ_0 [4,5], the conductivity measurements directly yield $g(E_F)$.

In Fig. 1 we report the *in situ* conductivity measurements at RT (a) and 77 K (b) during and after ion irradiation of an *a*-Si sample previously annealed at 813 K. Irradiations were performed by a 2.0 MeV Si beam at an ion flux of 1×10^{11} ions/cm^{2}sec. This beam passes completely through the 0.33 μm thick *a*-Si layer depositing a nearly constant energy and the layer is therefore made uniformly defective. In both cases the conductivity in-

0031-9007/93/70(24)/3756(4)$06.00
© 1993 The American Physical Society

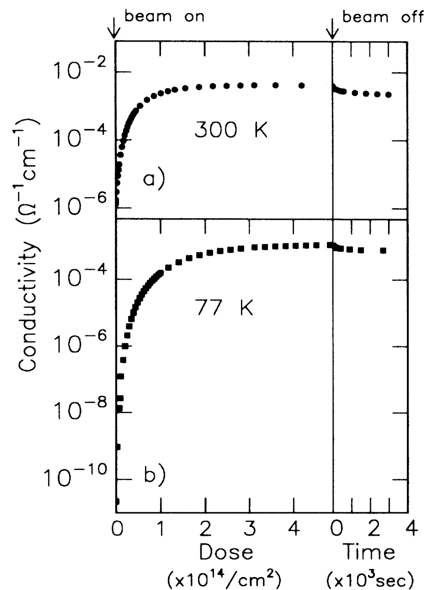

FIG. 1. *In situ* conductivity measurements of relaxed a-Si irradiated by 2.0 MeV Si ions at a dose rate of 1×10^{11} ions/cm^{2}s. The conductivity changes after turning off the beam are also shown on the right-hand side vs time. Data for 300 K (a) and 77 K (b) irradiations are shown.

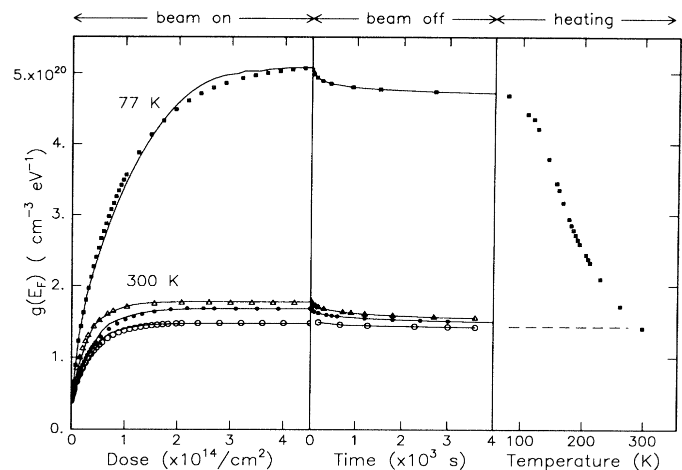

FIG. 2. DOS at the Fermi level [$g(E_F)$] during and after irradiation of relaxed a-Si samples, as deduced from conductivity measurements. On the left, $g(E_F)$ is reported vs dose under different irradiation conditions: 2.0 MeV Si, 1×10^{11}/cm^{2}s at 77 K (■) and at RT (●); 2.0 MeV Si, 2×10^{10}/cm^{2}s at RT (○); 7 MeV Au, 2×10^{10}/cm^{2}s at RT (△). In the center the beam is turned off and $g(E_F)$ is followed as a function of time. On the right, the evolution of $g(E_F)$ vs annealing temperature from 77 to 300 K is shown. The continuous lines are fits to the data.

creases due to the production of defects and eventually saturates. On turning off the beam, a small reduction in conductivity is observed, lasting for times as long as 1 h. In particular, at RT (a) the conductivity increases from an initial value of 1.3×10^{-6} to 4.1×10^{-3} Ω^{-1}cm^{-1}, which reduces to 1.3×10^{-3} Ω^{-1}cm^{-1} 1 h after turning off the beam. At 77 K (b) the initial conductivity value is much smaller, 1.4×10^{-11} Ω^{-1}cm^{-1}, due to the temperature dependence of the conductivity, and then saturates to 1.0×10^{-3} Ω^{-1}cm^{-1}. This value decreases to 7.1×10^{-4} Ω^{-1}cm^{-1} 1 h after turning off the beam. It should be noted that, since not only the irradiations but also the conductivity measurements are performed at two very different temperatures, similar conductivity values in the two measurements correspond to very different values in $g(E_F)$ [according to Eqs. (1) and (2)].

We have repeated similar measurements under different experimental conditions and converted the conductivity data into DOS at the Fermi level according to Eqs. (1) and (2). These results are shown in Fig. 2. The initial value of $g(E_F)$ (4×10^{19}cm^{-3} eV^{-1}, typical for a relaxed material) increases upon irradiation and eventually saturates, suggesting that a balance between defect production and annihilation occurs. It is evident that the effect of substrate temperature is quite dramatic. In fact, under irradiation with 2.0 MeV Si at a dose rate of 1×10^{11}/cm^{2}sec, the saturation value of $g(E_F)$ is 5.1×10^{20} cm^{-3}eV^{-1} at 77 K (■) and a factor of 3 lower at RT (●). This demonstrates that the defect structure of the material under irradiation is strongly dependent upon temperature. Moreover, at a fixed temperature (RT), changing the dose rate or the irradiating ion produces changes in the conductivity by less than a factor of 2, which correspond to only slight modifications in the DOS. In fact, for 2.0 MeV Si a reduction in the dose rate from 1×10^{11} (●) to 2×10^{10}/cm^{2}sec (○) reduces the DOS saturation value by only 10%. Furthermore, at a fixed dose rate of 2×10^{10}/cm^{2}sec passing from 2.0 MeV Si (○) to 7.0 MeV Au (△) (with an increase by a factor of 20 in the energy deposited into elastic collisions) produces an increase in the saturation value by only 15%. More extensive investigations have shown that this saturation value increases slightly but monotonically with the rate of energy deposition into elastic collisions while it does not depend on electronic excitations.

Turning off the beam, a small reduction in $g(E_F)$ lasting for ~1 h is observed. This demonstrates that annealing of the defects occurs even at 77 K on a long time scale. In particular, at 77 K a final equilibrium value of 4.8×10^{20} cm^{-3}eV^{-1} is observed, while at RT the final equilibrium value is a factor of 4 smaller and is basically independent of the irradiation conditions. This provides clear experimental evidence that the amount of defects and/or the defect structure obtained by ion implantation at 77 K strongly differ from those of a-Si produced by implantation at RT.

We have studied the annealing kinetics of these defects by turning off the beam at different values of $g(E_F)$ (well before saturation) and measuring the transient which followed. We have found that the annealing rate of defects

scales with the square of the defect density at the turn-off point demonstrating that a bimolecular kinetics is operative.

The use of an *in situ* technique allows us to follow the defect evolution upon heating from 77 K to RT. We have therefore slowly heated the sample, stopping the heating at different temperatures. At these temperatures, conductivity was measured after waiting for times of ~ 1 h to reach the equilibrium value. Each conductivity value was then converted into $g(E_F)$ using in Eqs. (1) and (2) a temperature T equal to that at which that value was actually measured. The results are shown on the right-hand side of Fig. 2 and demonstrate that dramatic defect annihilation occurs upon heating. It is interesting to observe that in spite of the large difference between the as-implanted states the defect density of a sample bombarded at 77 K and annealed up to RT is identical to that of samples directly bombarded at RT. This explains why *ex situ* techniques failed to observe this difference since they require heating of the sample to RT before analysis. These data make possible a more comprehensive description of structural relaxation in *a*-Si, since we can now follow the process from 77 K to the crystallization temperature. In Fig. 3(a) the equilibrium DOS at the Fermi level is reported from 77 to 900 K. In this figure the data between 300 and 900 K have been obtained by annealing the samples at the reported temperature and extracting $g(E_F)$ afterwards from the RT conductivity of the annealed samples. It should be observed that the decrease in $g(E_F)$ (i.e., the defect reduction) above 300 K is only a very limited portion of the phenomenon since most of the structural relaxation occurs actually below RT. The fact that at each temperature a different equilibrium value of $g(E_F)$ exists, demonstrates the presence of defects with a continuous spectrum of activation energies [22]. At a certain temperature, only those defects with accessible activation energies, are annealed out. The distribution of defects $D(E_a)$ in the spectrum can be obtained by a standard analysis [22] of the data in Fig. 3(a) and is reported in Fig. 3(b). The activation energy scale was obtained from the relationship

$$E_a = k_B T \ln(\nu t) , \quad (3)$$

ν being the attempt frequency and t a typical annealing time. For t a value of 3600 sec has been used while for the attempt frequency we have chosen a typical value of 1×10^{13} sec^{-1}. A similar value for ν has been previously used [2,4] in the description of relaxation phenomena in *a*-Si and changes in this parameter will only slightly affect the activation energy since ν enters in a logarithm in Eq. (3).

On the basis of the data of Fig. 3(b) several important conclusions may be reached. First, two different defect structures exist, with a well-defined range of activation energy. At energies above 1.5 eV, a Gaussian-like distribution peaked at 2.2 eV is observed in agreement with

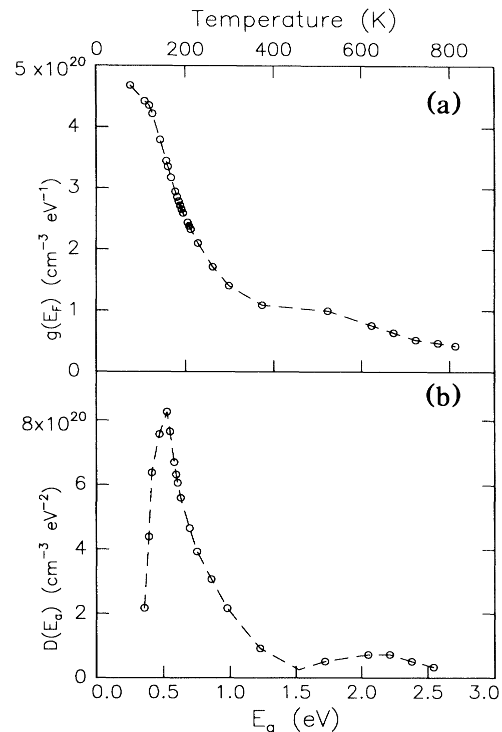

FIG. 3. (a) Equilibrium DOS at the Fermi level vs annealing temperature. (b) Activation energy spectrum for defects in *a*-Si as obtained from an analysis of part (a).

previous determinations by calorimetric [2] and conductance [4] measurements. However, most of the events are concentrated between 0.3 and 1 eV. This portion of the spectrum has never been observed before and is due to those defects which anneal out below RT. It should be noted that the energy released in the recombination events above RT has been measured by calorimetry [2] and corresponds to ~ 0.04 eV/atom. Since many more defects anneal out below RT the energy release associated with these recombination events is expected to be quite high and its determination would be interesting. According to the difference in activation energies we can speculate that the low energy portion of $D(E_a)$ is due to highly strained Si bonds, while the high energy region is due to broken Si-Si bonds. Moreover, the experimental observation that for each activation energy a well-defined limited number of defects exists [according to Fig. 3(b)] implies that defect accumulation can proceed until a maximum value in their concentration is reached.

The experimental data so far reported are a pathway towards understanding the mechanisms of defect production and recombination in *a*-Si. We propose the following scenario. An ion entering *a*-Si produces within its collision cascade a variety of defects distributed into different activation energies [according to Fig. 3(b)]. The process is intracascade and in the time interval be-

tween the arrival of two successive ions in the same region τ_0 the defects will move and will recombine in pairs. These assumptions are those proposed by Jackson [23] in explaining the process of ion-beam induced crystallization of a-Si. In that case, defects with a fixed activation energy of 1.2 eV were assumed while here the whole activation energy spectrum must be considered. According to their activation energy, and depending on the substrate temperature, defects can be divided into three classes. Defects having $E_a \ll k_B T \ln(\nu t)$ (class A) will be so mobile that they are fully recombined within τ_0. Therefore at that temperature they will play no role. Defects having $E_a \gg k_B T \ln(\nu t)$ (class B) are practically immobile and their population remains unchanged within τ_0. At the arrival of the next ion these defects will therefore accumulate until their maximum concentration is reached. Above this limit these defects can no longer be generated. Defects with $E_a \sim k_B T \ln(\nu t)$ (class C) will partially recombine within τ_0. At the arrival of the next ion their population will increase. However, due to their bimolecular recombination kinetics, a balance will be reached between generation and annihilation. The overall defect concentration (classes $B+C$) then reaches a saturation value, as experimentally observed (see Fig. 2). This value will critically depend upon temperature, since at lower temperatures larger portions of the defect spectrum can accumulate (i.e., more defects belong to class B). Moreover, changing the irradiating ion or dose rate will modify the balance between generation and annihilation for defects of class C, and thus their saturation value. However, since these defects represent only a small portion of the total amount of accumulating defects, the effect on the overall saturation value will be small. Moreover, turning off the beam can only produce the recombination of defects belonging to class C according to a bimolecular kinetics. All of these observations are in agreement with the data of Fig. 2. This model can also be quantitatively compared with the experimental data as shown in Fig. 2 (solid lines). The fits were made assuming that each ion produces N_0 defects, with a constant production over the activation energy spectrum. These defects undergo bimolecular recombination over the interval τ_0, according to the equation

$$\frac{dN}{dt} = -a\sigma^2 \nu e^{-E_a/kT} N^2 , \tag{4}$$

a being the lattice parameter, σ^2 the capture cross section, and ν the attempt frequency. For the product $a\sigma^2\nu$ we have chosen the literature value of 3×10^{-7} cm^2/s as proposed by Jackson [23]. The calculated defect densities were scaled into $g(E_F)$, dividing them by ΔW, the width of the band of deep-lying states introduced by the defects around the Fermi level. We have chosen a plausible value of 0.25 eV for ΔW. It is remarkable that all the fits were obtained by using a unique fitting parameter N_0 (1×10^{19}/cm^3). The agreement is excellent, demonstrating that the model is able to describe all the features of the experimental data, giving a plausible and comprehensive description of defect evolution in a-Si.

This work has been performed using the equipment of the CNR-IMETEM Laboratory in Catania. We wish to thank J. M. Poate and E. Rimini for several useful comments and A. Marino and A. Giuffrida for technical assistance.

[1] W. C. Sinke, T. Warabisako, M. Miyao, T. Tokuyama, S. Roorda, and F. W. Saris, J. Non-Cryst. Solids **99**, 308 (1988).
[2] S. Roorda, W. C. Sinke, J. M. Poate, D. C. Jacobson, S. Dierker, B. S. Dennis, D. J. Eaglesham, F. Spaepen, and F. Fuoss, Phys. Rev. B **44**, 3702 (1991).
[3] J. E. Frederickson, C. N. Waddell, W. G. Spitze and G. K. Hubler, Appl. Phys. Lett. **40**, 172 (1982).
[4] J. H. Shin and H. A. Atwater (to be published).
[5] S. Coffa, F. Priolo, J. M. Poate, and S. H. Glarum, Nucl. Instrum. Methods (to be published).
[6] S. Roorda, S. Doorn, W. C. Sinke, P. M. L. O. Scholte, and E. van Loenen, Phys. Rev. Lett. **62**, 1880 (1989).
[7] E. P. Donovan, F. Spaepen, J. M. Poate, and D. C. Jacobson, Appl. Phys. Lett. **55**, 1516 (1989).
[8] S. Coffa, J. M. Poate, D. C. Jacobson, W. Frank, and W. Gustin, Phys. Rev. B **45**, 8355 (1992).
[9] S. Roorda, J. M. Poate, D. C. Jacobson, B. S. Dennis, S. Dierker, and W. C. Sinke, Appl. Phys. Lett. **56**, 2097 (1990).
[10] W. G. Spitzer, G. K. Huber, and T. A. Kennedy, Nucl. Instrum. Methods **209/210**, 309 (1983).
[11] S. T. Pantelides, Phys. Rev. Lett. **58**, 1344 (1987).
[12] S. Coffa and J. M. Poate, Appl. Phys. Lett. **59**, 2296 (1991).
[13] G. N. van den Hoven, Z. N. Liang, L. Nielsen, and J. S. Custer, Phys. Rev. Lett. **68**, 3714 (1992).
[14] F. Priolo and E. Rimini, Mater. Sci. Rep. **5**, 319 (1990).
[15] J. S. Im and H. A. Atwater, Appl. Phys. Lett. **57**, 1766 (1990).
[16] C. Spinella, A. Battaglia, F. Priolo, and S. U. Campisano, Europhys. Lett. **16**, 313 (1991).
[17] F. Priolo, J. M. Poate, D. C. Jacobson, J. L. Batstone, and S. U. Campisano, Appl. Phys. Lett. **52**, 1213 (1988); S. Coffa, J. M. Poate, D. C. Jacobson, and F. Priolo, Appl. Phys. A **54**, 481 (1992).
[18] C. A. Volkert, J. Appl. Phys. **70**, 3521 (1991).
[19] C. A. Volkert (to be published).
[20] N. F. Mott and E. A. Davis, *Electronic Processes in Non-Crytalline Materials* (Oxford Univ. Press, Oxford, 1979).
[21] G. Müller and S. Kalbitzer, Philos. Mag. B **38**, 241 (1978).
[22] M. R. J. Gibbs, J. E. Evetts, and J. A. Leake, J. Mater. Sci. **18**, 278 (1983).
[23] K. A. Jackson, J. Mater. Res. **3**, 1218 (1988).